Journal of Wind Engineering and Industrial Aerodynamics, 46 & 47 (1993) 315–325
Elsevier

High Resolution Vortex Simulation of Bluff Body Flows

A. LEONARD

Professor of Aeronautics, Graduate Aeronautical Laboratories, California Institute of Technology, Pasadena, CA 91125, U.S.A.

P. KOUMOUTSAKOS

Graduate Research Assistant, Graduate Aeronautical Laboratories, California Institute of Technology, Pasadena, CA 91125, U.S.A.

Abstract

New advances in vortex methods for the simulation of unsteady incompressible flows, the fast-vortex algorithm for convection and the method of particle-strength exchange for viscous diffusion, are discussed. The application to bluff body flows is demonstrated for transient flows past a circular cylinder for Re = 40 to 9500.

1. INTRODUCTION

Advancements in vortex methods for bluff body flows are continuing at a rapid pace. They remain as an interesting serious alternative to finite difference or finite volume approaches. The advantages of vortex methods are well known - (1) computational elements are needed only where the vorticity is nonzero, (2) rigorous treatment of the boundary conditions at infinity is a natural byproduct and, (3) physical insights gained by dealing directly with the vorticity field. Interesting examples go back more than 30 years. In these studies, for example, useful insights concerning Strouhal frequency and unsteady lift and drag for high Reynolds number two-dimensional flow were obtained using reasonable assumptions about the locations of separation points and just a few vortices [1] or even only two vortices [2]. For more discussion and examples see Sarpkaya [3].

Until recently, two major problems with vortex methods, limiting their widespread use, have been (1) the requirement of $\mathcal{O}(N^2)$ operations per timestep for N computational elements which had excluded the possibility of pushing the method to high accuracy even though computer speeds have increased dramatically and (2) the accurate treatment of viscous effects.

In this paper we describe recent advances that remove the restrictions above, the fast-vortex algorithm and the method of particle-strength exchange, and present some applications based on implementing these new developments. For most of the paper we will be discussing the case of two-dimensional flow. The extension of our work to three dimensions is proceeding rapidly and will be the subject of a forthcoming paper.

2. VISCOUS VORTEX METHOD

2.1 Vortex Particles

In the present method the vorticity field is represented by a collection of moving computational elements with locally distributed vorticity ($\boldsymbol{\omega} = \omega \hat{\mathbf{e}}_z$) and variable circulation as follows,

$$\omega(\mathbf{x}, t) = \sum_{i=1}^{N} \Gamma_i(t)\, \eta_\sigma(\mathbf{x} - \mathbf{x}_i(t)) \tag{1}$$

where Γ_i is the circulation, η is the distribution for each particle, and σ is the width of the distribution. The velocity field $\mathbf{u}(\mathbf{x}, t)$ is given by the solution to

$$\nabla^2 \mathbf{u} = -\nabla \times \boldsymbol{\omega} \tag{2}$$

yielding

$$\mathbf{u} = -\frac{1}{2\pi} \int \frac{(\mathbf{x} - \mathbf{y}) \times \boldsymbol{\omega}(\mathbf{y})}{|\mathbf{x} - \mathbf{y}|^2}\, d\mathbf{y} + \mathbf{U}_\infty(t) \tag{3}$$

where we have included the free-stream component of the velocity as a solution to the homogeneous equation (2). No additional potential flow is required because all the vorticity in the flow is assumed to be carried by the particles, including the vorticity in the boundary layers.

We wish to find evolution equations for $\mathbf{x}_i(t)$ and $\Gamma_i(t)$, satisfying as accurately as possible the vorticity transport equation,

$$\frac{\partial \boldsymbol{\omega}}{\partial t} + \mathbf{u} \cdot \nabla \boldsymbol{\omega} = \nu \nabla^2 \boldsymbol{\omega} \tag{4}$$

with the boundary conditions for a stationary body given by

$$\mathbf{u}|_{\text{surface}} = 0 \tag{5a}$$

and

$$\mathbf{u} \to \mathbf{U}_\infty \qquad \text{as} \quad |x| \to \infty \tag{5b}$$

Using the momentum equation at the surface and the requirement (5a), we obtain an equation for the vorticity flux through the body surface,

$$\nu \frac{\partial \omega}{\partial n} = -\frac{1}{\rho} \frac{\partial p}{\partial s} \tag{6}$$

where s and n are local tangential (clockwise) and normal coordinates on the surface and p and ρ are the pressure and density.

2.2 Particle Velocity

Substituting the particle representation (1) into the vorticity transport equation (4), we obtain

$$\sum_{i=1}^{N} \frac{d\Gamma_i}{dt}\,\eta \;+\; \sum_{i=1}^{N} \Gamma_i\,(-\frac{d\mathbf{x}_i}{dt} \;+\; \mathbf{u}(\mathbf{x}))\cdot\,\nabla\eta \;=\; \nu \sum_{i=1}^{N} \Gamma_i \nabla^2 \eta \tag{7}$$

The i-th term in the summations above is only significantly nonzero in a neighborhood of size σ of the point $\mathbf{x} = \mathbf{x}_i(t)$. Thus the second summation in (7) can be made approximately zero by the choice,

$$\frac{d\mathbf{x}_i}{dt} \;=\; \mathbf{u}(\mathbf{x}_i) \tag{8}$$

For a variety of simple choices of the distribution η (e.g., gaussian) the error is $\mathcal{O}(\sigma^2)$ with the proviso that the typical interparticle distance, h, satisfies $h < \sigma$. Higher order schemes are possible (see [4,5] for more details). Here $\mathbf{u}(\mathbf{x}_i)$ is determined by substituting (1) into (3) to obtain

$$\frac{d\mathbf{x}_i}{dt} \;=\; -\frac{1}{2\pi}\sum_{j=1}^{N} \Gamma_j\,\frac{(\mathbf{x}_i - \mathbf{x}_j)\times \widehat{\mathbf{e}_z}}{|\mathbf{x}_i \;-\; \mathbf{x}_j|^2}\; g(|\mathbf{x}_i \;-\; \mathbf{x}_j|/\sigma) \;+\; \mathbf{U}_\infty(t) \tag{9}$$

where

$$g(y) \;=\; 2\pi \int_0^y \eta(z)\, z\, dz \tag{10}$$

2.3 Viscous Diffusion

For viscous diffusion we need to update the vorticity field, on the particle locations, following the equation

$$\frac{d\omega}{dt} \;=\; \nu\nabla^2\omega \tag{11}$$

with the boundary condition (6). The random walk method, as discussed by Chorin [6], has been applied widely for a number of years but has the disadvantage of being slowly convergent. More recently the technique of particle strength exchange (see Degond and Mas-Gallic [7]) has been proposed. This method has good convergence properties but requires an occasional remeshing of the particles as discussed below. In this algorithm we approximate ∇^2 as an integral operator and discretize the integration over the particles. Thus, we use

$$\nabla^2\omega \;\approx\; G \,*\, \omega \;=\; \frac{1}{\sigma^2}\int G(|\mathbf{x}-\mathbf{y}|/\sigma)\,[\omega(\mathbf{y}) \;-\omega(\mathbf{x})]\,d\mathbf{y} \tag{12}$$

where, for example, with gaussian particle distributions,

$$G(z/\sigma) \;=\; 4\eta(z/\sigma) \;=\frac{4}{\pi\sigma^2}\; exp(-|z|^2/\sigma^2) \tag{13}$$

Consider first the application to an infinite domain. The approximation (12) is good to second order in σ as we can see by taking the Fourier transform of both sides,

$$-k^2\,\hat{\omega} \;=\; \frac{4}{\sigma^2}[exp(-k^2\sigma^2/4)-1]\hat{\omega} \;=\; -k^2\hat{\omega}(1 \;+\; \mathcal{O}(k^2\sigma^2)) \tag{14}$$

Using (12) and the particle representation we find that (Eq.11) can be written

$$\sum_i \frac{d\Gamma_i}{dt}\,\eta(\frac{|\mathbf{x}-\mathbf{x}_i|}{\sigma}) \;=\; \frac{\nu}{\sigma^2}\int G(|\mathbf{x}\;-\;\mathbf{y}|/\sigma) \\ [\sum_j \Gamma_j\eta(\frac{|\mathbf{y}-\mathbf{x}_j|}{\sigma}) \;-\; \sum_i \Gamma_i\eta(\frac{|\mathbf{x}-\mathbf{x}_i|}{\sigma})]\;d\mathbf{y} \tag{15}$$

Note now that by approximating the integral on the right hand side of (15) over the particles and using (13) we obtain the evolution equation for the problem in an infinite domain,

$$\frac{d\Gamma_i}{dt} \;=\; \frac{\nu\,h^2}{\sigma^2}\sum_j G(|\mathbf{x}_i\;-\;\mathbf{x}_j|/\sigma)(\Gamma_j\;-\;\Gamma_i) \tag{16}$$

where h^2 is the particle area.

The above algorithm conserves circulation exactly, i.e., $\sum_i^N d\Gamma_i/dt \;=\; 0$. It is found that if (16) is integrated in time with Euler timestepping and

$$\Delta t \;=\; \frac{\sigma^2}{\nu} \tag{17}$$

then the results are superaccurate. This phenomenon may be explained by noting that the exact solution to (11) at time $t+\Delta t$ is given by

$$\omega(\mathbf{x},t+\Delta t) \;=\; \int \frac{exp(-|\mathbf{x}-\mathbf{y}|^2/4\nu\Delta t)}{4\pi\nu\Delta t}\,\omega(\mathbf{y},t)\;d\mathbf{y} \tag{18}$$

For wall-bounded flows, we enforce the no-slip condition at each time step by evaluating the vorticity flux at the surface of the body. The surface of the body is approximated by a vortex sheet, whose strength ($\gamma(s)$) is determined by enforcing the no-through flow boundary condition. This vortex sheet implies a tangential velocity on the surface of the body. To enforce then the no-slip boundary condition this vortex sheet diffuses into the fluid with a vorticity flux given by :

$$\nu\frac{\partial\omega}{\partial n}(s) \;=\; -\frac{\gamma(s)}{\Delta t} \tag{19}$$

This flux is then distributed to the particles by discretizing the Greens' integral for the inhomogeneous Neumann problem for the diffusion equation [9].

2.4 Remeshing

In order for the numerical simulation to be accurate, the particles must, to a certain degree, be uniformly distributed. This is required for accuracy in the convection step as well as the diffusion step. On the other hand the local strain following a particle may generate a substantial contraction or crowding of particles in one direction accompanied by an expansion in another direction, similar to the situation at a hyperbolic stagnation point in steady flow. When remeshing is deemed necessary we overlay a regular grid (the new particles) over the old particles, keeping the average particle density constant, and interpolate the old vorticity onto the new particle locations. We use a nine-point scheme to distribute the old vorticity to the new mesh. Specifically, away from a wall, the ith old vortex with circulation Γ_i and location $(x_i,\ y_i)$ contributes $\Delta\Gamma_{j,i}$ circulation to new mesh point $(\tilde{x}_j, \tilde{y}_j)$ according to

$$\Delta\Gamma_{j,i} \ = \ \Gamma_i \, \Lambda(\frac{\tilde{x}_j \ - \ x_i}{h}) \, \Lambda(\frac{\tilde{y}_j \ - \ y_i}{h}) \tag{20}$$

where the interpolation kernel Λ is given by

$$\Lambda(u) \ = \ \begin{cases} 1 \ - \ u^2, & 0 \ \leq \ |u| \ < \ 1/2; \\ (1 \ - \ u)(2 \ - \ u)/2, & 1/2 \ \leq \ |u| \ < \ 3/2; \\ 0, & \text{otherwise.} \end{cases} \tag{21}$$

If the old particle is less then a distance h from a wall the interpolation is modified to maintain the same conservation properties. See [9,10] for further discussion. This scheme conserves the circulation, linear and angular momentum.

2.5 Fast Vortex Method

The straightforward method of computing the right hand side of (Eq.8), using (Eq.9) for every particle, requires $\mathcal{O}(N^2)$ operations for N vortex elements. This precludes high resolution studies of bluff body flows with more than say 50,000 elements.

Recently fast methods (see e.g., [11],[12]) have been developed that have operation counts of $\mathcal{O}(N\log N)$ or $\mathcal{O}(N)$ depending on the details of the algorithm. The basic idea of these methods is to decompose the element population spatially into clusters of particles and build a hierarchy of clusters ("tree") - smaller neighboring clusters combine to form a cluster of the next size up in the hierarchy and so on. Fig. 1 shows an example of particle clustering.

The contribution of a cluster of particles to the velocity of a given vortex can then be computed to desired accuracy if the particle is sufficiently far from the cluster in proportion to the size of the cluster and a sufficiently large number of terms in the multipole expansion is taken. This is the essence of the particle/box (PB) method, requiring $\mathcal{O}(N\log N)$ operations. One then tries to minimize the work required by maximizing the size of the cluster used while keeping the number of terms in the expansion within a reasonable limit and maintaining a certain degree of accuracy.

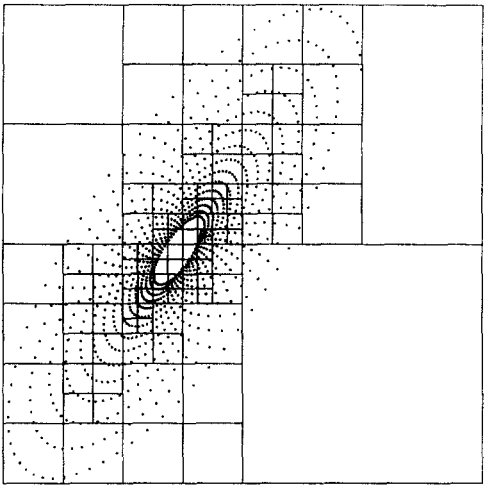

FIG. 1 Example of particle clustering for an elliptical spiral distribution of 1000 particles.

The box-box (BB) scheme goes one step further as it accounts for box-box interactions as well. These interactions are in the form of shifting the expansions of a certain cluster with the desired accuracy to the center of another cluster. Then those expansions are used to determine the velocities of the particles in the second cluster. This has as an effect the minimization of the tree traversals for the individual particles requiring only $\mathcal{O}(N)$ operations.

In our present implementation on a Cray XMP and YMP great care was taken with regard to vectorization [9]. Both the PB and the BB method were implemented as well as the N^2 method. Fig. 2 shows the CPU time required on a single processor of an XMP in each of the three methods for an evaluation of all N velocities for N elements with a minimum accuracy of 10^{-6}. Note that fast methods become advantageous for computations involving only $N \approx 500$ particles with the BB method beating out the PB method for $N \approx 4400$. The time required on a YMP processor is about 2/3 of the time required on an XMP. A timestep requiring one evaluation of all velocities for a million particles requires about one minute on single processor of a CRAY YMP while the N^2 algorithm would require roughly 24 hours.

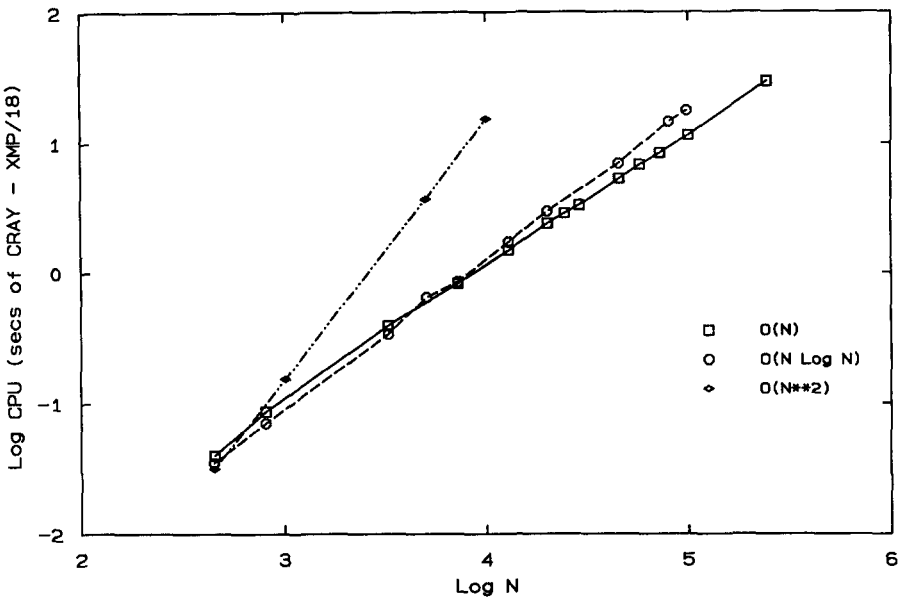

FIG. 2 Computational Cost of the PB, BB and direct summation algorithms

2.6 Results

In Fig.3 we show drag coefficients versus non-dimensional time ($t = U_\infty T/R$) for an impulsively started flow past a circular cylinder (with radius R) for various Reynolds numbers. Also shown are theoretical results [13,14], valid for asymptotically small time. The comparisons indicate that the present method is able to handle a large range of Re number. In Fig.4 and Fig.5 we show vorticity contours, streamlines and experimental short exposure streaklines for $Re = 550$ at time $t = 5$ and for $Re = 9500$ at time $t = 3$ respectively, again for an impulsively started flow. Note that the vorticity distribution is clearly more complex for the higher Re number case.

2.7 Summary

It was shown that fast vortex algorithms coupled to a new technique for treating viscous diffusion in vortex methods, the method of particle strength exchange, produce a powerful tool for studying bluff-body flows by accurate numerical simulations. The present demonstrations were in two dimensions on a vector computer. We are now concentrating on three dimensional methods and applications and implementation on parallel computers.

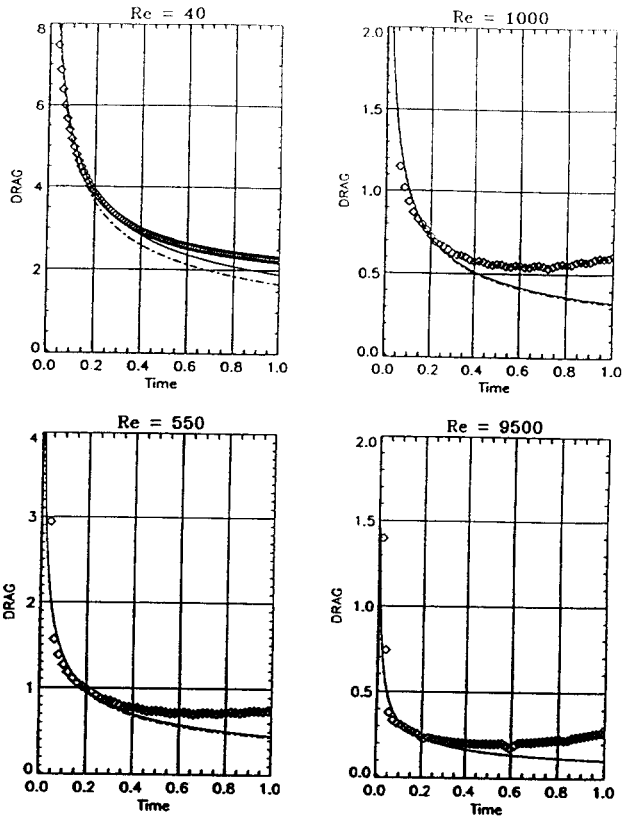

FIG. 3 Comparison of drag coefficient for various *Re* numbers, with theoretical results of [13] (dashed line) and [14](solid line).

2.8 Acknowledgements

We are pleased to acknowledge the support of this research by the Office of Naval Research through Grant Nos. N00014-92-J-1072 and N00014-92-J-1189. Computer time was provided by Caltech's Jet Propulsion Laboratory Supercomputing Project.

References

1. Kiya, M and A. Arie. "A contribution to an inviscid vortex-shedding model for an inclined flat plate in uniform flow". *J. Fluid Mech.* Vol. 82, (1977), pp. 241-253.

2. Bryson, A.E.. "Symmetric Vortex Separation on circular cylinders and cones". *J. Appl. Mech.* Vol. 26, (1959), pp. 643-648.

3. Sarpkaya, T.. "Computational methods with vortices - The 1988 Freeman scholar lecture". *ASME J. Fluids Eng.* Vol. 111, (1988), pp. 5-52.

4. Leonard, A.. "Vortex Methods for flow simulation". *J. Comp. Phys.* Vol. 37, (1980), pp. 289-335.

5. Beale, J.T. and A. Majda. "Vortex methods II : High order accuracy in two and three dimensions". *Math. Comp.* Vol. 39, (1982), pp. 29-52.

6. Chorin, A. "Numerical study of slightly viscous flow". *J. Fluid Mech.* Vol. 57, (1973), pp. 380-392.

7. Degond, P. and S. Mas-Gallic. "The weighted particle method for convection-diffusion equations, Part I: the case of isotropic viscosity, Part II: the anisotropic case". *Math. Comp.* Vol. 53, (1989), pp. 485-526.

8. Pepin, F. ,1990. *Simulation of the flow past an impulsively started cylinder using a discrete vortex method*. Ph.D. thesis, Caltech.

9. Koumoutsakos, P. ,1992. *Direct Numerical Simulations of Unsteady Separated Flows Using Vortex Methods*. Ph.D. thesis, Caltech.

10. Hockney, R.W. and J.W. Eastwood . *Computer simulations using particles*. McGraw-Hill, New York, 1981.

11. Barnes, J.E. and P. Hut. "A hierarchical $\mathcal{O}(N\log N)$ force calculation algorithm.". *Nature* Vol. 324, (1986), pp. 446-449.

12. Greengard, L. and V. Rohklin. "A Fast Algorithm for particle simulations". *J. Comp. Phy.* Vol. 73 (1987), pp. 325-348.

13. Collins, W.M. and S.C.R. Dennis. "The Initial flow past impulsively started circular cylinder . *Quart. J. Mech and Appl. Math.* Vol. 26 (1973), pp. 53-75.

14. Bar-Lev, M. and H.T. Yang. "Initial flow field over an impulsively started circular cylinder . *J. Fluid Mech.* Vol. 72 (1975), pp. 625-647.

15. Bouard, R. and M. Coutanceau. "The early stage of development of the wake behind an impulsively started cylinder for $40 \leq 10^4$.. *J. Fluid Mech.* Vol. 101 (1980), pp. 583-608.

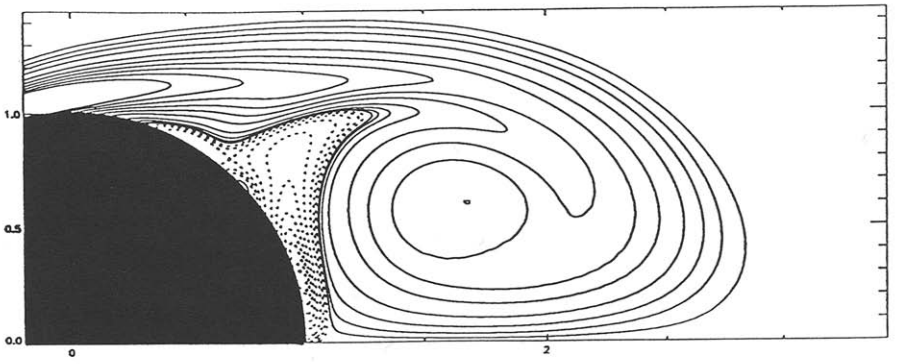

(a) Vorticity
(Computations)

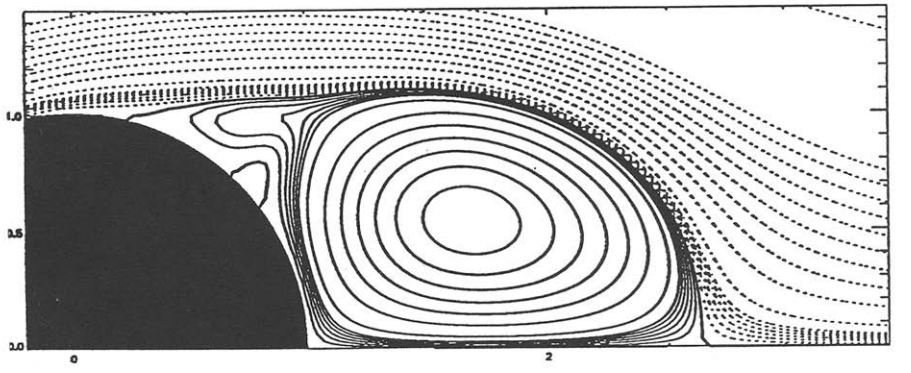

(b) Streamlines
(Computations)

(c) Streaklines
(Experiments)

Fig. 4 Comparison of experimental flow visualization [15] and present computations for $Re = 550, t = 5$.

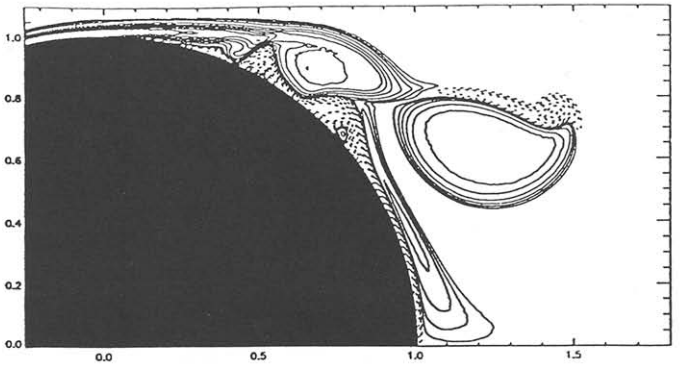

(a) Vorticity

(Computations)

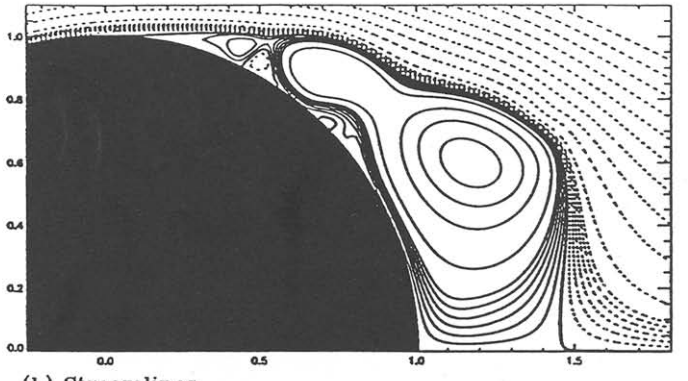

(b) Streamlines

(Computations)

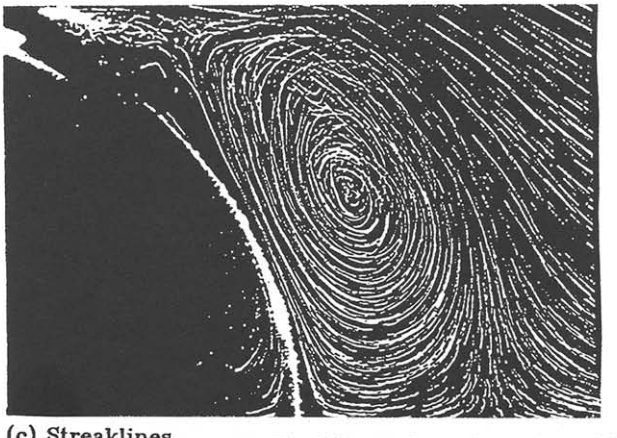

(c) Streaklines

(Experiments)

Fig. 5 Comparison of experimental flow visualization [15] and present computations for $Re = 9500, t = 3$.